In Vitro and in Vivo Comparative Study of a Novel 68 Ga-Labeled PSMA-Targeted Inhibitor and 68 Ga - PSMA-11

Huanyu Chen
Affiliated Hospital of Southwest Medical University
Ping Cai
Affiliated Hospital of Southwest Medical University
Yue Feng
Affiliated Hospital of Southwest Medical University
Zhanliang Sun
Affiliated Hospital of Southwest Medical University
Yinwen Wang
Affiliated Hospital of Southwest Medical University
Yue Chen
Affiliated Hospital of Southwest Medical University
Nan Liu
Affiliated Hospital of Southwest Medical University
Zhijun Zhou (zhouzjiang@gmail.com)
Affiliated Hospital of Southwest Medical University
Wei Zhang
Affiliated Hospital of Southwest Medical University

Research Article

Keywords: prostate-specific membrane antigen, prostate cancer, positron emission tomography, inhibitor, 68Ga(), LNCaP

Posted Date: March 25th, 2021

DOI: https://doi.org/10.21203/rs.3.rs-347420/v1

Abstract

^{68}Ga-radiolabeled small molecules that specifically target prostate specific membrane antigen (PSMA) has been extensively investigated, and some of those tracers have been used in diagnosis of prostate cancer with ^{68}Ga-positron emission tomography (^{68}Ga-PET). Nevertheless, current ^{68}Ga-labeled radiotracers show fair detection rates to metastasized prostate cancer lesions, especially to those with lower level of prostate specific antigen (PSA), which often occur in biochemical recurrence of prostate cancer. The goal of this study was to design and synthesize a new PSMA-targeted radiotracer ^{68}Ga-SC691 with high affinity to prostate cancer cells and excellent pharmacokinetics. To this end, structural optimum was made on the bifunctional group, target motif, and linker while high affinity targeting scaffold was remained. In order to explore its potential in clinical, a comparative study was further performed *in vitro* and *in vivo* between ^{68}Ga-SC691 and ^{68}Ga-PSMA-11, the clinically approved tracer for PSMA-positive prostate cancer. SC691 was radiolabeled to provide ^{68}Ga-SC691 in 99% radiolabeling yield under mild conditions. High uptake and internalization ratio into LNCaP cells were observed in *in vitro* studies. In vivo studies showed that ^{68}Ga-SC691 had a favorable biodistribution property and can specifically accumulate on PSMA-positive LNCaP xenografts visualized by micro-PET/CT. This radiotracer showed excellent PET imaging quality and comparable uptake at LNCaP xenografts if not higher than ^{68}Ga-PSMA-11.

Introduction

Prostate cancer (PCa) is the most common cancer form in males in the United States. It is estimated that there will be more than 190,000 new cases of prostate cancer and an estimated 33,000 deaths from this disease in USA only in 2020, according to the National Cancer Institute[1]. Statistically, even though prostate cancer cells in most PCa cases remain locally, about 10% of total number of PCa patients will suffer from metastasis or biochemical recurrence[2]. Advanced techniques such as Computed Tomography (CT) and Magnetic Resonance Imaging (MRI) provide high contrast and resolution, however, imaging outcomes from these methods often suffer from either short of functional information or explicit explanation from corresponding professionals needed[3–5]. As well, they find difficulty in detecting microscale lesions, which are often observed in postoperative examinations. Positron Emission Tomography (PET) as a functional imaging method, together with targeting radiotracers, has been widely used in clinical due to its precision and ultrahigh sensitivity[6]. To date, PET/CT and PET/MRI fusing imaging as novel multimodality technology combining benefits of anatomic information from CT or MRI scan imaging and functional information from PET, have become one of the most powerful imaging methods in disease diagnosis and single cell tracking[7,8].

PCa possesses unique pathophysiologic and biological characteristics. A great number of studies found that overexpression of transmembrane protein, namely prostate specific membrane antigen (PSMA), also known as glutamate carboxypeptidase, dominates in over 90% prostate carcinoma and tumor-associated endothelium of various solid cancer tissue[9,10]. Along with other properties, such as over 94% amino acids

of the transmembrane protein locating outside of membrane[11], PSMA has become one of the most extensively studied drug targets and shows prominent promise in the prostate cancer cell detection[12–14].

Even though macromolecules like antibodies were introduced a few decades ago[15], due to the outstanding merits of small molecules such as pure substance, definitive structure, and clear structure-activity-relationship, small molecule PSMA inhibitors have been mostly investigated[16]. According to targeting scaffold, small molecule PSMA inhibitors fall into three major families: (1) thiols[17]; (2) phosphonate-, phosphate-[18], and phosphoramidates; and (3) ureas[19]. Among these inhibitors, small molecules with Glu-urea-Lysine scaffold as a pharmacophore was found to be able to accumulate on prostate cancer cells specifically and efficiently. Thus, a series of Glu-urea-Lysine-based PSMA-targeted imaging agents with favorable biological properties emerged to visualized PCa lesions, such as ^{18}F-DCFPyL, ^{18}F-PSMA-1007, ^{68}Ga-PSMA-11[20], and ^{68}Ga-PSMA-617[21–24] (Fig. 1). Until now, no PET agents have been approved for clinical use in PCa diagnosis except for ^{68}Ga-PSMA-11, which was approved in December 2020[25]. Unlike ^{18}F-radiolabeled tracers, which need cyclotron to produce ^{18}F and complex procedure and facility to be applied for synthesis of ^{18}F-radiopharmaceuticals, the readily availability, efficient complexing characteristic of ^{68}Ga(Ⅲ), together with its favorable biological properties make ^{68}Ga-based, PSMA-targeted PET procedures grow rapidly evidenced by increasing number of clinical trials[26–30]. Among them, ^{68}Ga-PSMA-11 is the mostly investigated and the only approved PCa radiotracer by FDA. And now it is being routinely used in diagnosis, treatment evaluation, and staging of PCa.

Herein, we present the synthesis and *in vitro* and *in vivo* study of a novel and PSMA-targeted radiotracer ^{68}Ga-SC691. We further evaluated its affinity and specificity to PSMA positive tumor by comparing its pharmacokinetics and PET imaging with ^{68}Ga-PSMA-11. It turned out that ^{68}Ga-SC691 displayed favorite pharmacokinetics and excellent uptake at PSMA positive tumor, indicating that ^{68}Ga-SC691 may serve as a new PET tracer for prostate cancer.

Results

- Chemical, Radiochemical Synthesis and Characterization

We firstly constructed the urea-based **b-3** scaffold bearing protected glutamine and lysine followed by hydrogenation to provide **b-4** with a combined yield of 51.1%. Converting **b-4** into **b-6** must be paid attention to the ratio of reactants, otherwise, a disubstituted compound will dominate in the products instead of the monosubstituted compound **b-6. b-6** was produced with a yield of 77.7%. With **b-6** in hand, we further substitute secondary amine into tertiary amine **b-8** with *para*-iodo benzoyl moiety. After reduction of **b-8**, conjugation between **a** and **b** was performed to provide **TM-1.** The target molecule SC691 was obtained via deprotection of TM-1 in dilute acid with a yield of 39.1% (Scheme 1, Figure S1, Figure S2). The multistep reactions were conducted with a total yield of 2.8%.

Radiolabeling of SC691 with ^{68}Ga() eluate is straightforward. It may be performed in NaAc/HAc buffer or HEPES buffer (pH 4.0–5.0) under ambient temperature to 95°C in high radiolabeling yield (~ 95–99%) and radiochemical purity (> 98%) after purification analyzed using analytic RP-HPLC (equipped with a gamma detector) with specific activity as high as 18.8 MBq/μg (Fig. 2). The retention time has increased from 9.9 min to 10.4 min after SC691 radiolabeled with ^{68}Ga (). In the cased of PSMA-11 and ^{68}Ga-PSMA-11, the retention time were 8.7 min and 9.0 min, respectively. Thus, SC691 displayed a longer retention time on HPLC and extended retention time was observed for both precursor upon radiolabeling.

- Lipophilicity and stability

We further investigated the hydrophilicity and stability of ^{68}Ga-SC691. The partition coefficient (Log P) between octane and Phosphate buffered saline (PBS) is usually used to measure hydrophilicity of a compound. It turned out that ^{68}Ga-SC691 and ^{68}Ga-PSMA-11 had Log P values being − 3.530 ± 0.086 and − 2.91 ± 0.06[31], respectively (Table 1). These data indicated that ^{68}Ga-SC691 is more hydrophilic than ^{68}Ga-PSMA-11. Stability study of ^{68}Ga-SC691 were performed both in PBS and in fetal bovine serum (FBS) at 37 ℃. The radiotracer showed time-dependent stability in both systems, but in a 2 h duration, excellent stability was revealed as it was indicated by over 96% of ^{68}Ga-SC691 remaining unchanged in retention time of analytical radio-HPLC (Fig. 3).

Table 1
Analytical data of SC691, ^{nat}Ga-SC691, and PSMA-11.

Compound code	Chemical formula	MW [g/mol]	m/z[1]	tr [min]	Radiochemical purity [%]	Log D
SC691	$C_{43}H_{68}IN_8O_{17}$	1092.92	1093.3472	9.91	N.A.	N.A.
^{nat}Ga-SC691	$GaC_{43}H_{65}IN_8O_{17}$	1159.05	N.A.	10.11	99%[2]	-3.530 ± 0.086[3]
PSMA-11	$C_{44}H_{62}N_6O_{17}$	946.99	947.4257	9.04	96%[5]	-2.91 ± 0.06[4]

[1] Mass spectrometry data detected as $[M + H]^+$.

[2] Value for radiochemical purity measured by RP-HPLC. Agilent analytical column (250 x 4.6 mm) utilized with mobile phases consisting of 0.1% TFA in water (A) and ACN (B). For analytical runs, a linear gradient of solvent A (90 − 10% in 15 min) in solvent B at a flow rate of 1.0 mL was used for a 15 min run.

[3] Obtained from ^{68}Ga-SC691. See the detailed description of the method in materials and method.

[4] This value is for ^{68}Ga-PSMA-11 from literature[31].

[5] The purity of PSMA-11 was taken from the ABX GmBH certificate of this compound.

Another important aspect of a radiopharmaceutical is the radiochemical stability, which determines whether a radioligand is worth carrying out further *in vivo* and *in vitro* studies or not. ^{68}Ga-SC691 showed excellent stability both in PBS and in FBS incubated for 2 hours at 37 ℃. By the end of 2-hour incubation in PBS and FBS, ^{68}Ga-SC691 still maintained its radiochemical purity 97.9% and 97.5%, respectively.

- Cell Affinity Studies

Uptake and internalization experiments of ^{68}Ga-SC691 in LNCaP cells revealed high uptake and internalization rate. Internalization and uptake of ^{68}Ga-SC691 displayed a time-dependent pattern and maintained increasing trend for 120 min. Interestingly, uptake of ^{68}Ga-SC691 nearly reached saturation at 60 min, and only a slight increase was observed. On the other hand, its internalization experienced relatively fast increase in the whole experimental period. A blocking experiment with 2-PMPA was conducted to demonstrate the specificity of ^{68}Ga-SC691 toward PSMA *in vitro*. It turned out that cell uptake of ^{68}Ga-SC691 can be nearly completely blocked with 2-PMPA (data not shown).

- Biodistribution

The results of biodistribution study of ^{68}Ga-SC691 in LNCaP mice bearing prostate cancer (NOD/SCID) was decay-corrected and listed as percentage of the injected activity per gram of tissue mass (% ID/g) and presented as the average ± standard deviation (SD). As summarized in Fig. 5, organ distribution with ^{68}Ga-SC691 revealed a high specific uptake in LNCaP tumor being 43.41 ± 8.39 %ID/g at 30 min and 27.59 ± 10.38 %ID/g at 60 min. High accumulation of radioactivity maintained over 2 hours measurements (observed from micro-PET/CT). Similar trend in uptake was observed for the kidneys.

The uptake of ^{68}Ga-SC691 was shown to be specific by the co-injection of ^{68}Ga-SC691 together with 2-PMPA, demonstrating reduced tumor uptake by 30.55 %ID/g at 60 min post injection (12.86 ± 2.80 %ID/g, n = 2). Biodistribution studies of ^{68}Ga-SC691 also demonstrated pronounced uptake in kidneys and slight uptake in liver, probably suggesting both hepatobiliary and kidney excretion pathways, but kidneys show much higher uptake of ^{68}Ga-SC691 over liver suggesting that kidneys contributed most significantly and thus the principal excretion organs. Tumor-to-background ratios were determined as 5.86 (tumor / blood) and 34.49 (tumor / muscle), respectively, 1 h post injection. It is consistent with other PSMA-specific radioligands that no significantly reduced uptake except for kidneys occurred in normal organs as it was seen in blocking experiments.

- Micro-PET/CT imaging

Next, whole body micro-PET/CT imaging was studied for ^{68}Ga-SC691 and ^{68}Ga-PSMA-11 (as a reference) in intact male NOD/SCID mice (Fig. 6) bearing LNCaP tumor only or bearing both LNCaP and PC-3 tumors in opposite, upper flanks (Fig. 7, Figure S4). Static imaging method was applied to both compounds with time points at 5 min, 30 min, 60 min, and 120 min. Following the static PET scan, a dynamic PET scan was conducted to understand time-dependent pharmacokinetic of ^{68}Ga-SC691

(Fig. 8). As a result of both static and dynamic scan, these radiotracers were able to visualize the PSMA-positive LNCaP tumor as early as 5 min post injection but not the PC-3 tumor. Micro-PET/CT images and dynamic uptake curve clearly showed the fast-targeting property and high retention rate of ^{68}Ga-SC691 at the tumor site during the 2-hour experiment, which was consistent with the biodistribution results. Besides tumor, uptake of other organs such as heart and kidneys became evident during the initial 5 minutes, and uptake in heart was diminished at 30 minutes and thereafter. The comparative PET/CT imaging also clearly showed that ^{68}Ga-SC691 had a similar renal clearance with ^{68}Ga-PSMA-11. Quantitative data from micro-PET/CT showed that the mean %ID/g at tumor for both ^{68}Ga-SC691 and ^{68}Ga-PSMA-11 kept increasing up to 2 hours post injection and a rapid elimination of radioactivity occurred from other organs, muscle, and blood (with a quite clear background). But the uptake curve became flatter with time as summarized in Fig. 8A. In comparison to ^{68}Ga-PSMA-11, ^{68}Ga-SC691 displayed similar uptake both in tumor and in kidneys.

Discussion

PSMA is strongly overexpressed on prostate cancer cells and therefore is selected as one of the most important drug targets for prostate cancer diagnosis, staging, and follow-up. PSMA inhibitors, after radiolabeled with ^{68}Ga presents favorable properties as availability and facile complexation chemistry. Here we report the successful synthesis of ^{68}Ga-SC691 via multistep chemical reactions and complexation with ^{68}Ga (□) method. To date, Lys-Urea-Glu has become the most common and important targeting motif of PSMA inhibitor structure due to its high affinity and specificity to PSMA. To manage the pharmaceutical and metabolic properties of desired tracers, amide or secondary amine linker produced by Lys is the most popular strategy while keeping Lys-Urea-Glu untouched. Until 2019, Banerjee and coworkers reported the first case of the tertiary amination modification strategy of the amino group on Lysine side chain modified by *p*-halo benzyl moiety and obtained several PSMA inhibitors with high binding affinity and excellent *in vivo* properties, which opened a precedent for tertiary amination modification strategy[32,33]. Inspired by quite low *Ki* value of the compound *iodo*-DCFPyL (Fig. 1) (*Ki* = 0.01 nmol), we decided to introduce *p*-iodo benzoyl moiety into Lysine on the Lys-Urea-Glu scaffold to verify the possibility to obtain a PSMA inhibitor with a high affinity through the tertiary amination strategy. On the other hand, the macrocyclic chelating agent with four acetate donor arms was demonstrated *in vitro* and *in vivo* a higher tumor uptake and retention, thus DOTAGA other than DOTA was selected as the chelating agent due to its favorable property. A shorter or longer linker with number of methylene groups > 4 was reported to yield no significant impact on tumor uptake and retention. Together with chelating agent and *p*-iodo benzoyl moiety, SC691 was finalized to be expected excellent *in vitro* and *in vivo* properties.

The synthesis of SC691 is quite straight forward except for the step involving the conversion of primary amine into secondary amine, in which dimer was resulted. To enhance the yield of monosubstituted product, molar ratio and temperature should be carefully controlled. In contrast to DOTA, DOTAGA has one more carboxylic acid group providing an extra complexation site to Ga(□). The complexation

chemistry of DOTAGA is more facile than DOTA, so that it can be carried out at lower temperature while achieving high radiochemical yield. This tracer was quite stable in PBS buffer and FBS with over 96% intact compound in both media after 2 hours incubation at 37 ℃.

To improve precision with regard to comparison, a further purification with HPLC to remove unlabeled precursor (SC691 or PSMA-11) was applied. Specificity for ^{68}Ga-SC691 was confirmed by its high uptake in PSMA-positive LNCaP cells and by blocking experiments in a LNCaP-inoculated NOD/SCID mouse model (Figure S3). The accumulated radioactivity was not seen on PC-3 tumor but on LNCaP tumor. Upon co-injection of the PSMA inhibitor 2-PMPA, uptake of ^{68}Ga-SC691 was completely blocked, so that quite low radioactivity was detected, which indicated that the novel tracer had an exceptional specificity for PSMA-positive tumor. Biodistribution also showed that the tumor is the major site and kidneys played a critical role as the more important excretion organ compared with liver. Tumor retention of ^{68}Ga-SC691 maintained at a high level over 2 hours post injection, which is consistent with *in vitro* cell uptake and internalization. Interestingly, chelator DOTAGA exerted an evident impact on the properties of ^{68}Ga-SC691 by changing its lipophilicity or charges. In particular, the pharmacological property was strong influenced by the more hydrophilic ^{68}Ga-SC691.

The results obtained from micro-PET/CT imaging experiments indicated ^{68}Ga-SC691 had a slightly higher absolute uptake than ^{68}Ga-PSMA-11 in PSMA-positive tumor (Fig. 8A). To be noticed, an unexpected and longer blood clearance was observed for ^{68}Ga-SC691 considering that ^{68}Ga-SC691 is much more hydrophilic than ^{68}Ga-PSMA-11 (Table 1). We proposed that structural modification not only changed its hydrophilicity but also changed its binding affinity with plasma protein, such as albumin. To confirm that, serum albumin binding experiment was carried out and demonstrated that introducing *p*-iodo benzoyl moiety clearly enhanced its affinity to serum albumin thus extended its circulation time in blood (data not shown). This property of longer blood circulation is favored for therapeutic agents if no safety issue exists. With regard to diagnostic agents, higher accumulation at targeted organs could also be beneficial in practice due to extended blood circulation as diagnostic dose of radioactivity generally does not yield significant adverse reactions but potentially improve precision prognosis.

Materials And Methods

- Precursor Synthesis

Synthetic route and chemical structures of SC691 and ^{68}Ga-SC691 were shown in scheme 1. Synthesis of SC691 is quite straightforward through multi-step reactions and SC691 was purified with preparative high performance liquid chromatography (prep-HPLC). The detailed synthesis is attached in the supporting information.

- ^{68}Ga-radiolabeling

Typically, 5~20 μL of SC691 (1 mg/mL in pure water) was added in a volume of 100 μL sodium acetate/acetic acid (NaAc/HAc) buffer (NaAc/HAc = 0.5 M / 0.5 M, pH = 4.45), followed by a 400 μL ^{68}Ga(Ⅲ) eluate (18.5 -40 MBq). The reaction mixture was incubated at 80 °C for 10 min. The radiochemical purity was determined by reverse phase-HPLC (RP-HPLC).

- ^{nat}Ga-complexation

A 20 times molar excess of ultrapure ^{nat}Ga(Ⅲ)-Chloride (Aladdin, China) in NaAc/HAc (pH = 4.45, NaAc/HAc = 0.5 M/0.5 M, both ultrapure grade) (400 μL) and HCl (0.05 M, 1600 μL) was reacted with the compounds SC691 (1 mg/mL) for 8 hours at 80 °C. The reaction mixture was purified via preparative RP-HPLC and the product was obtained as white solid after lyophilization.

- Radiochemical stability

The stability studies were carried out by incubating ^{68}Ga-SC691 at 37 ℃ for 30 min, 60 min, and 120 min either in PBS buffer or in FBS. At each time point, radiochemical purity was directly analyzed using RP-HPLC for samples in PBS buffer. While samples in FBS were pretreated before it could be analyzed. Briefly, the FBS samples were precipitated with acetonitrile, followed by centrifugation for 5 min at 10,000 rpm. The aliquots of supernatant of FBS samples were determined using RP-HPLC.

- Cell binding studies

Cell binding studies were performed using PSMA positive LNCaP cell line. LNCaP cells were cultured in Gibco RPMI 1640 medium supplemented with 10% FBS and 1% Streptomycin/Penicillin (from ThermoFisher Scientific, US). Cells were grown at 37 ℃ for 24 h in an incubator with humidified air and equilibrated with 5% CO_2. One day prior to the experiment, after removal of medium, cells were washed off with trypsin-ethylenediaminetetraacetic acid (EDTA, 0.25% Trypsin, 0.02% EDTA) and PBS. Cells were resuspended in above medium and dispersed in 24-well plates and incubated under above conditions for 24 h. The cells were washed with PBS, followed by addition of 450 μL Gibco RPMI 1640 and 50 μL of the corresponding radioligand to each well. The well-plates were then incubated for 10 min, 30 min, 60 min and 120 min. To determine the uptake of the added radioactivity, the cells were washed three times with ice-cold PBS and lysed with 100 μL 1 M NaOH. The internalized fraction was determined in cells, which were washed with ice-cold PBS, then incubated for 10 min with acidic stripping buffer (0.05 M glycine stripping buffer in 100 mM NaCl, pH 2.8) followed by an additional washing step with ice-cold PBS. All cell samples were measured with γ-counter (CAPRAC-t, Edmonton, Canada).

- Log D measurement

^{68}Ga-SC691 was aliquoted into vials of 500 μL octanol and 490 μL of 0.01 M PBS buffer (pH = 7.4). Each vial was vortexed for 5 min and centrifugated for 10 min (5000 rpm). Relative concentrations were determined with RP-HPLC (equipped with gamma counter) for octanol and PBS buffer samples (1 mL for

each sample). Log D was determined using the following equation: Log D = Log [(gamma counts in octanol phase) / (gamma counts in PBS phase)].

- Biodistribution and Imaging studies

Tumor model

Human prostate cancer cell lines LNCaP and PC-3 (PSMA-negative control) were obtained from the American Type Culture Collection (ATCC). Cells were counted and 5 x 10^6 cells of either LNCaP or PC-3 in 100 µL of RPMI-1640 were injected subcutaneously into male 4-5 weeks old non-obese diabetic/severe combined immunodeficiency (NOD/SCID) mice. Animals were grown under standard conditions 3 to 4 weeks to allow tumor to establish before biodistribution and imaging.

Biodistribution

Biodistribution studies were performed 3 to 4 weeks after LNCaP tumor cell inoculation when tumor xenografts reached an average mass about 20 ± 5 g corresponding to 5-8 mm in diameter of tumor. SC691 was radiolabeled with ^{68}Ga at a specific activity of ~24.5 MBq/nmol and diluted in sterilized saline (0.9% NaCl in DI water) to final specific activity around 2.8 MBq/nmol. Tumor-bearing were intravenously injected with 100 µL of ^{68}Ga-SC691 (~2.8 MBq). The mice were sacrificed at 30 min, 60 min, and 120 min post injection and important organs were collected, weighed, and radioactivity was measured with γ-counter (CAPRAC-t, Edmonton, Canada). Mice were grouped with specific time points and 3-5 mice in a group.

Imaging studies

The ^{68}Ga-radiolabeled compounds ^{68}Ga-SC691 were injected into the tail vein of the male mice bearing LNCaP and PC-3 tumors (~3.7 MBq; 100 µL). All animals were performed in prone position for micro-PET imaging at 5 min, 30 min, 60 min and 120 min post injection. During the imaging process, mice were anaesthetized and maintained under 2% isoflurane in oxygen at a flow rate of 2 L/min. The data analysis was used the Inveon Research Workplace software.

Conclusions

In summary, we report a novel and ^{68}Ga-labeled ligand for noninvasive detection of prostate cancer. This ligand showed a promising binding and internalization properties *in vitro* as well as high specific uptake and favorite retention time *in vivo*. This radiotracer showed excellent PET imaging quality and comparable uptake with ^{68}Ga-PSMA-11 at LNCaP xenografts if not higher. The feasibility of prostate cancer imaging with ^{68}Ga-SC691 is under evaluation on human.

Declarations

Acknowledgements

This research was funded by Doctoral Research Initiation Fund of Affiliated Hospital of Southwest Medical University, Nuclear Medicine and Molecular Imaging Key Laboratory of Sichuan Province (HYX19001), and Luzhou Science and Technology Achievement Transformation Platform (2019CGZHPT08), National Natural Science Foundation of China (U20A20384), and the Sichuan Science and Technology Foundation (2020ZYD101)

Author Contributions statement

Conceptualization, Z.Z.J.; methodology, Z.Z.J, N.L., and Y.C.; validation, N.L., H.Y.C. and P.C.; formal analysis, Z.Z.J.; investigation, H.Y.C., P.C., Z.L.S., Y.F., N.L., and Y.W.W.; resources, Y.C. and Wei Zhang; data curation, H.Y.C. and P.C.; writing, Z.Z.J.; funding acquisition, Z.Z.J. All authors reviewed the manuscript.

Institutional Review Board Statement: The study was approved by Ethics Committee for Animal of Southwest Medical University (2019-06-27).

All methods were carried out in accordance with relevant guidelines and regulations and all methods are reported in accordance with ARRIVE guidelines

Conflicts of Interest: The authors declare no conflict of interest.

References

1 Stephens, K. FDA OKs First PSMA-Targeted PET Imaging Drug for Men with Prostate Cancer. *AXIS Imaging News* (2020).

2 Artibani, W., Porcaro, A. B., De Marco, V., Cerruto, M. A. & Siracusano, S. Management of Biochemical Recurrence after Primary Curative Treatment for Prostate Cancer: A Review. *Urol. Int.***100**, 251-262, doi:10.1159/000481438 (2018).

3 Diwakar Manoj, K. M. A review on CT image noise and its denoising. *Biomed. Signal Process Control***42**, 73-88, doi:org/10.1016/j.bspc.2018.01.010 (2018).

4 Hyodo, T. *et al.* CT and MR cholangiography: advantages and pitfalls in perioperative evaluation of biliary tree. *Br. J. Radiol.***85**, 887-896, doi:org/10.1259/bjr/21209407 (2012).

5 Zhu, Y. *et al.* In Vivo Molecular MRI Imaging of Prostate Cancer by Targeting PSMA with Polypeptide-Labeled Superparamagnetic Iron Oxide Nanoparticles. *Int. J. Mol. Sci.***16**, 9573-9587, doi:10.3390/ijms16059573 (2015).

6 Boellaard, R. *et al.* FDG PET/CT: EANM procedure guidelines for tumour imaging: version 2.0. *Eur. J. Nucl. Med. Mol. Imaging* **42**, 328-354 (2015).

7 Ehman, E. C. *et al.* PET/MRI: where might it replace PET/CT? *Magn. Reson. Imaging* **46**, 1247-1262, doi:org/10.1002/jmri.25711 (2017).

8 Jung, K. O. *et al.* Whole-body tracking of single cells via positron emission tomography. *Nat. Biomed. Eng* **4**, 835-844, doi:org/10.1038/s41551-020-0570-5 (2020).

9 Susan D. Sweat, A. P., Gerald P. Murphy, And David G. Bostwick. Prostate-specific membrane antigen expression is greatest in prostate adenocarcinoma and lymph node metastasis. *Urology* **52**, 637-640, doi:org/10.1016/S0090-4295(98)00278-7 (1998).

10 Sam S. Chang, V. E. R., W. D. W. Heston, Neil H. Bander, Lana S. Grauer, and Paul B. Gaudin. Five Different Anti-Prostate-specific Membrane Antigen (PSMA) Antibodies Confirm PSMA Expression in Tumor-associated Neovasculature. *Cancer Res.***59**, 3192–3198 (1999).

11 Mesters, J. R. *et al.* Structure of glutamate carboxypeptidase II, a drug target in neuronal damage and prostate cancer. *EMBO J* **25**, 1375-1384, doi:10.1038/sj.emboj.7600969 (2006).

12 Donin, N. M. & Reiter, R. E. Why Targeting PSMA Is a Game Changer in the Management of Prostate Cancer. *J. Nucl. Med.***59**, 177-182, doi:10.2967/jnumed.117.191874 (2018).

13 Baratto, L. *et al.* PSMA-and GRPR-targeted PET: Results from 50 Patients with Biochemically Recurrent Prostate Cancer. *J. Nucl. Med.*, doi:10.2967/jnumed.120.259630 (2021).

14 Bravaccini, S. *et al.* PSMA expression: a potential ally for the pathologist in prostate cancer diagnosis. *Scientific reports* **8**, 1-8, doi:org/10.1038/s41598-018-22594-1 (2018).

15 He Liu, P. M., Sae Kim, Yan Xia, Ayyappan Rajasekaran, Vincent Navarro, Beatrice Knudsen, and Neil H. Bander. Monoclonal Antibodies to the Extracellular Domain of Prostate-specific Membrane Antigen Also React with Tumor Vascular Endothelium. *Cancer Res.***57**, 3629-3634 (1997).

16 Jones, W., Griffiths, K., Barata, P. C. & Paller, C. J. PSMA Theranostics: Review of the Current Status of PSMA-Targeted Imaging and Radioligand Therapy. *Cancers (Basel)***12**, 1367-1370, doi:10.3390/cancers12061367 (2020).

17 Tiancheng Liu, Y. T., Marat Kazak, and Clifford E. Berkman. Pseudoirreversible Inhibition of Prostate-Specific Membrane Antigen by Phosphoramidate Peptidomimetics. *Biochemistry* **47**, 12658–12660, doi:org/10.1021/bi801883v (2008).

18 Paul F. Jackson, D. C. C., Barbara S. Slusher,Susan L. Stetz, Laurie E. Ross,Bruce A. Donzanti, and Diane Amy Trainor. Design, Synthesis, and Biological Activity of a Potent Inhibitor of the Neuropeptidase N-Acetylated r-Linked Acidic Dipeptidase. *J. Med. Chem* **39**, 619-622, doi:org/10.1021/jm950801q (1996).

19 Ying Chen, C. A. F., Youngjoo Byun, Sridhar Nimmagadda, Mrudula Pullambhatla, James J. Fox, Mark Castanares, Shawn E. Lupold, John W. Babich, Ronnie C. Mease, and Martin G. Pomper.

Radiohalogenated Prostate-Specific Membrane Antigen (PSMA)-Based Ureas as Imaging Agents for Prostate Cancer. *J. Med. Chem.***51**, 7933–7943, doi:org/10.1021/jm801055h (2008).

20 Barakat, A. *et al.* Role of early pet/ct imaging with 68Ga-PSMA in Staging and Restaging of prostate cancer. *Scientific reports* **10**, 1-6, doi:org/10.1038/s41598-020-59296-6 (2020).

21 Chen, Y. *et al.* 2-(3-{1-Carboxy-5-[(6-[18F]fluoro-pyridine-3-carbonyl)-amino]-pentyl}-ureido)-pen tanedioic acid, [18F]DCFPyL, a PSMA-based PET imaging agent for prostate cancer. *Clin. Cancer Res.***17**, 7645-7653, doi:10.1158/1078-0432.CCR-11-1357 (2011).

22 Eder, M. *et al.* Novel Preclinical and Radiopharmaceutical Aspects of [68Ga]Ga-PSMA-HBED-CC: A New PET Tracer for Imaging of Prostate Cancer. *Pharmaceuticals (Basel)***7**, 779-796, doi:10.3390/ph7070779 (2014).

23 Dietlein, M. *et al.* Comparison of [(18)F]DCFPyL and [(68)Ga]Ga-PSMA-HBED-CC for PSMA-PET Imaging in Patients with Relapsed Prostate Cancer. *Mol. Imaging Biol.***17**, 575-584, doi:10.1007/s11307-015-0866-0 (2015).

24 Cardinale, J. *et al.* Preclinical Evaluation of (18)F-PSMA-1007, a New Prostate-Specific Membrane Antigen Ligand for Prostate Cancer Imaging. *J. Nucl. Med.***58**, 425-431, doi:10.2967/jnumed.116.181768 (2017).

25 Carlucci, G. *et al.* 68Ga-PSMA-11 NDA approval: a novel and successful academic partnership. *J. Nucl. Med.***62**, 149-155, doi:org/10.2967/jnumed.120.260455 (2021).

26 Afshar-Oromieh, A. *et al.* Comparison of PET imaging with a (68)Ga-labelled PSMA ligand and (18)F-choline-based PET/CT for the diagnosis of recurrent prostate cancer. *Eur J Nucl Med Mol Imaging* **41**, 11-20, doi:10.1007/s00259-013-2525-5 (2014).

27 Kuten, J. *et al.* Head-to-head comparison of 68Ga-PSMA-11 with 18F-PSMA-1007 PET/CT in staging prostate cancer using histopathology and immunohistochemical analysis as a reference standard. *J. Nuc. Med.***61**, 527-532, doi:org/10.2967/jnumed.119.234187 (2020).

28 von Eyben, F. E. *et al.* Optimizing PSMA Radioligand Therapy for Patients with Metastatic Castration-Resistant Prostate Cancer. A Systematic Review and Meta-Analysis. *Int. J. Mol. Sci.***21**, 9054-9070, doi:10.3390/ijms21239054 (2020).

29 Afshar-Oromieh, A. *et al.* Comparison of PET/CT and PET/MRI hybrid systems using a 68Ga-labelled PSMA ligand for the diagnosis of recurrent prostate cancer: initial experience. *Eur. J. Nucl. Med. Mol. Imaging* **41**, 887-897, doi:10.1007/s00259-013-2660-z (2014).

30 Afshar-Oromieh, A. *et al.* Diagnostic performance of (68)Ga-PSMA-11 (HBED-CC) PET/CT in patients with recurrent prostate cancer: evaluation in 1007 patients. *Eur. J. Nucl. Med. Mol. Imaging* **44**, 1258-1268, doi:10.1007/s00259-017-3711-7 (2017).

31 Baranski, A. C. *et al.* PSMA-11-Derived Dual-Labeled PSMA Inhibitors for Preoperative PET Imaging and Precise Fluorescence-Guided Surgery of Prostate Cancer. *J. Nucl. Med.***59**, 639-645, doi:10.2967/jnumed.117.201293 (2018).

32 K. P. Maresca, S. M. H., F. J. Femia, D. Keith, C. Barone, J. L. Joyal, C. N. Zimmerman, A. P. Kozikowski, J. A. Barrett, W. C. Eckelman, and J. W. Babich. A Series of Halogenated Heterodimeric Inhibitors of Prostate Specific Membrane Antigen (PSMA) as Radiolabeled Probes for Targeting Prostate Cancer. *J. Med. Chem.***52**, 347-357, doi:org/10.1021/jm800994j (2009).

33 Banerjee, S. R. *et al.* (177)Lu-labeled low-molecular-weight agents for PSMA-targeted radiopharmaceutical therapy. *Eur. J. Nucl. Med. Mol. Imaging* **46**, 2545-2557, doi:10.1007/s00259-019-04434-0 (2019).

Figures

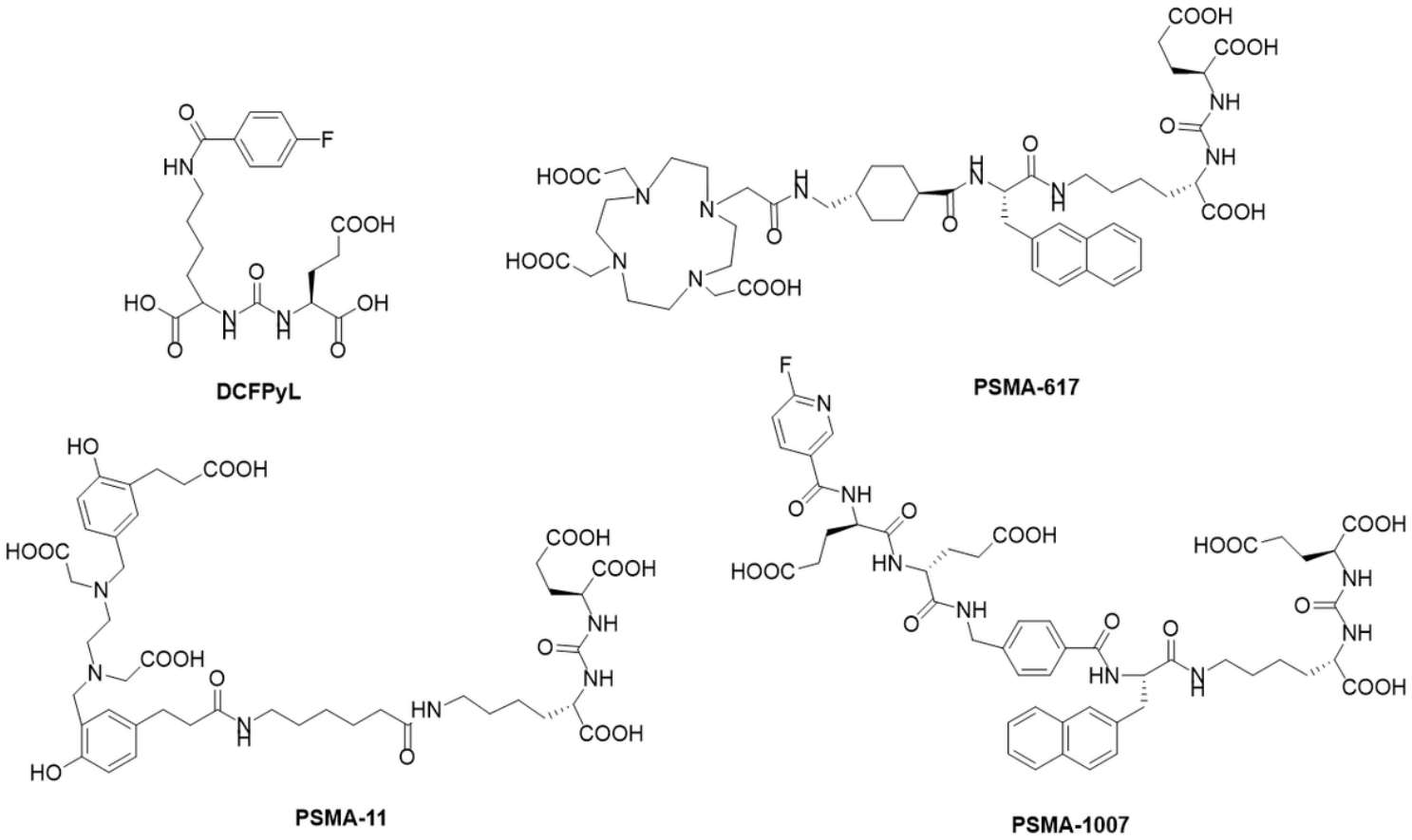

Figure 1

Most often-used precursors based on Lys-Urea-Glu scaffold for PCa detection

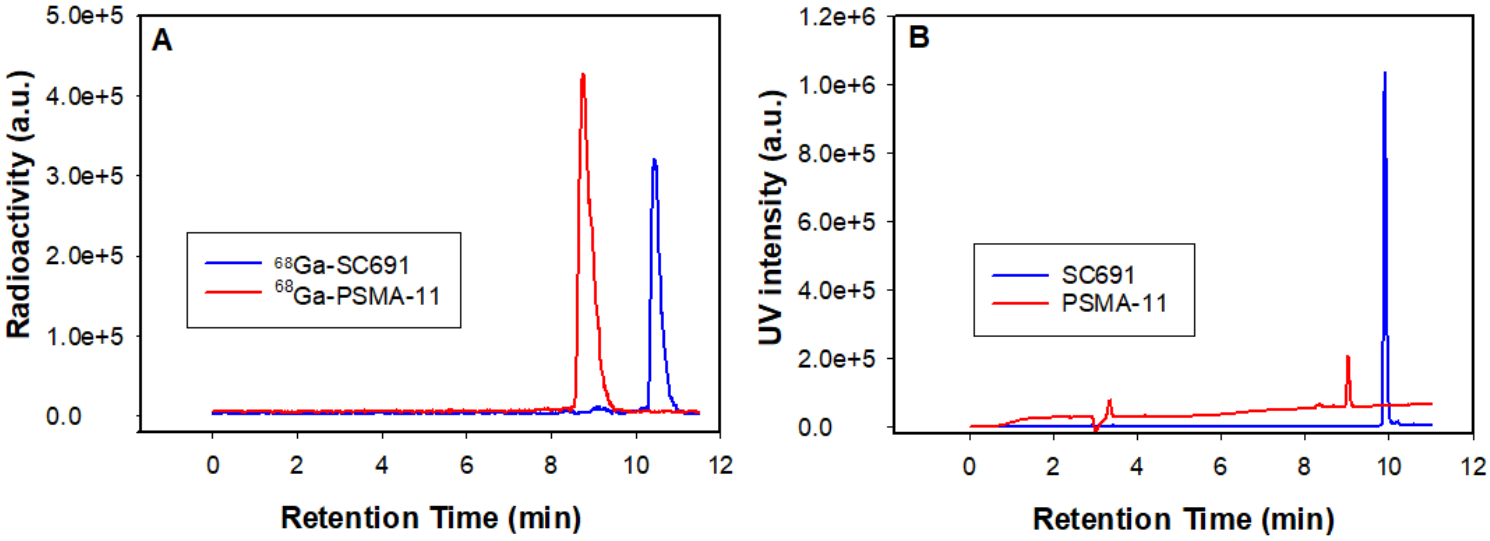

Figure 2

HPLC of 68Ga-PSMA-11(red line) and 68Ga-SC691(blue line) (A), and PSMA-11 (red line) and SC691(blue line) (B)

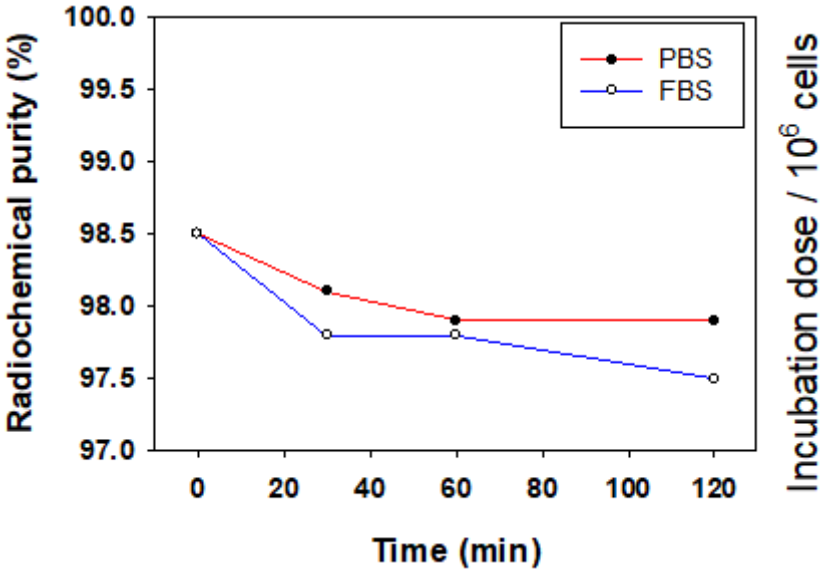

Figure 3

Stability of 68Ga-SC691. Radiochemical purity was recorded in PBS and FBS at 0 min (initial point), 30 min, 60 min, 120 min.

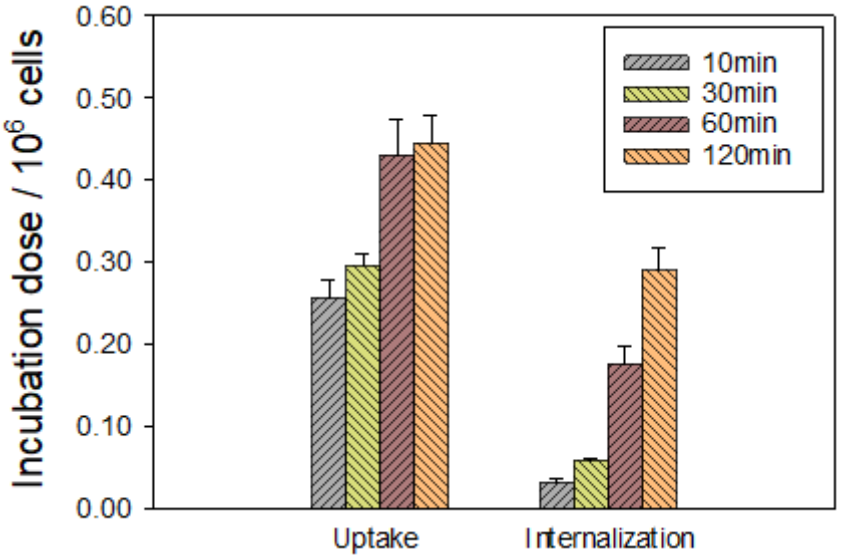

Figure 4

The uptake and internalization of 68Ga-SC691 in LNCaP cells (~200,000 cells/well, normalized to 106 cells) at 10 min, 30 min, 60 min, and 120 min.

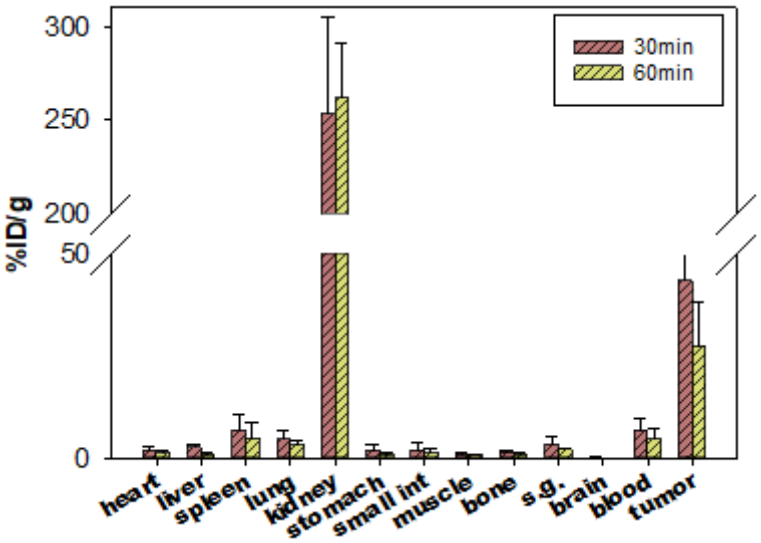

Figure 5

Organ Biodistribution of 68Ga-SC691 expressed as %ID/g tissue 30 min and 60 min post injection. Data are expressed as mean ± SD (n = 3). s.g. = salivary glands, small int = small intestine.

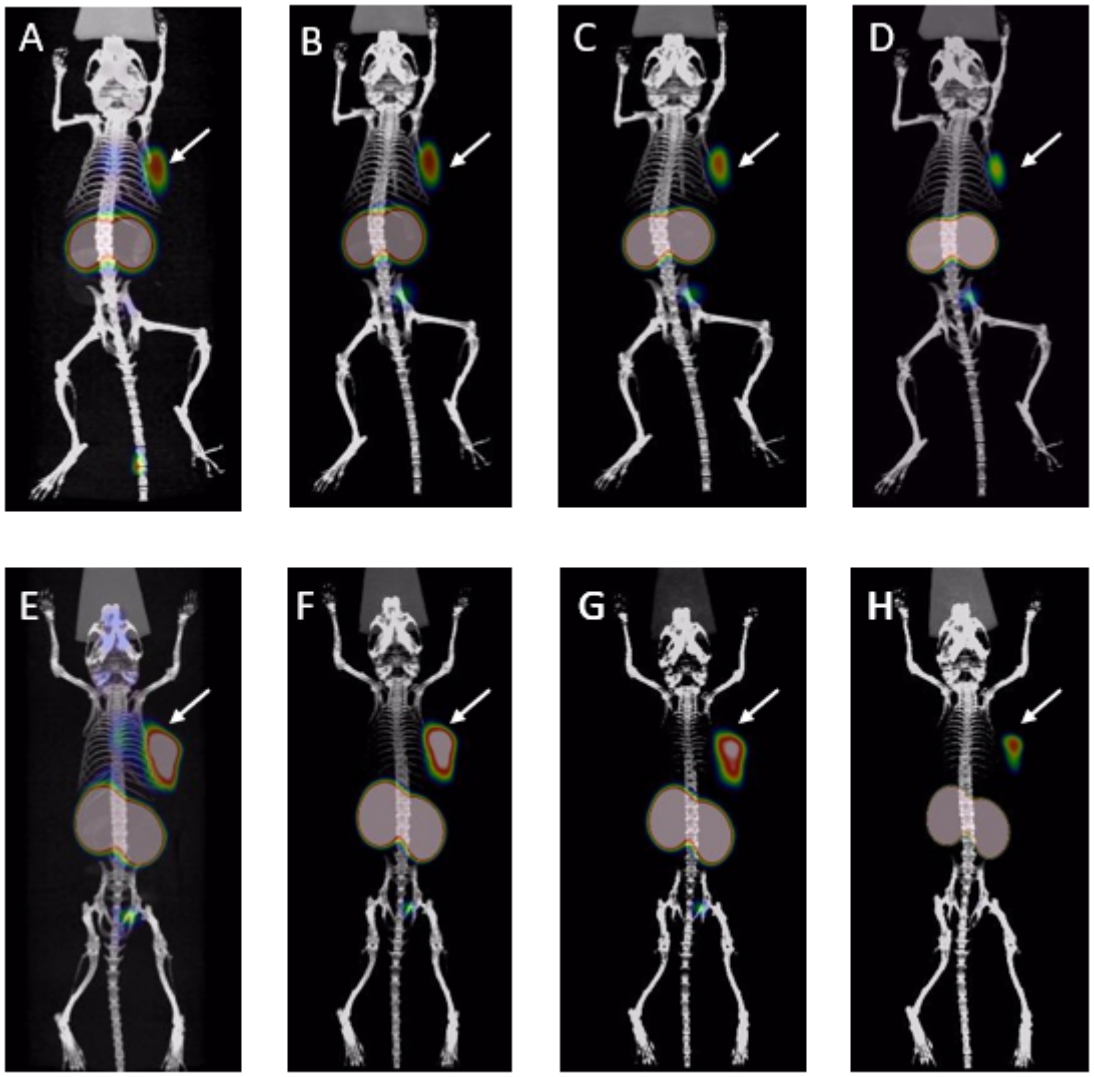

Figure 6

Maximum intensity projection of whole-body coronal micro-PET/CT images of an NOD/SCID male mouse bearing LNCaP tumor xenografts (white arrow). The tumor targeting efficacy of 68Ga-SC691 and 68Ga-PSMA-11 was demonstrated by time-dependent static scan at 5 min, 30 min, 60 min, 120 min post injection of 68Ga-SC691 (A,B,C,D) and 68Ga-PSMA-11 (E,F,G,H). Approximately 1.9 MBq/ mouse was injected.

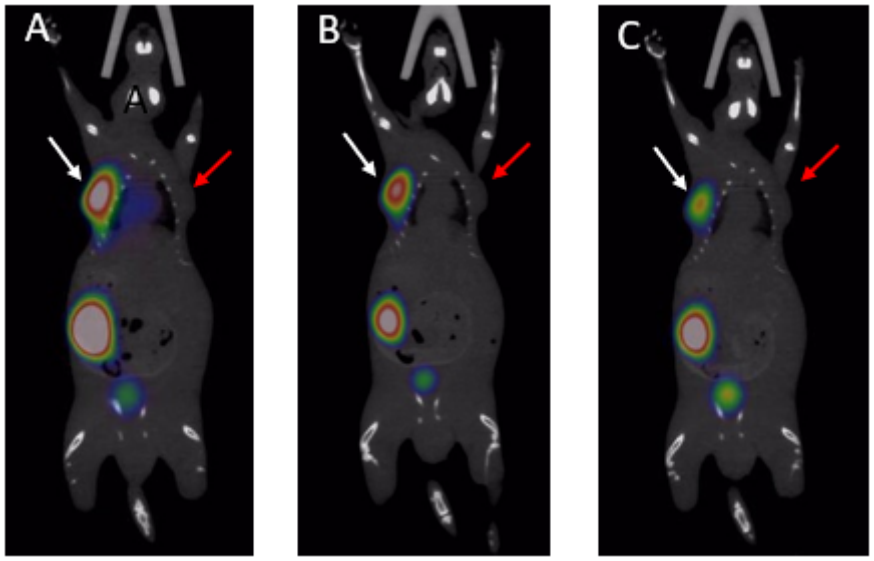

Figure 7

Whole-body coronal micro-PET/CT images of an NOD/SCID male mouse bearing LNCaP tumor xenografts in PC-3 and LNCaP inoculated xenografts (LNCaP on the left with white arrow, PC-3 on the right with red arrow) post injection of 68Ga-SC691. A) 30 min, B) 60 min, C) 120min.

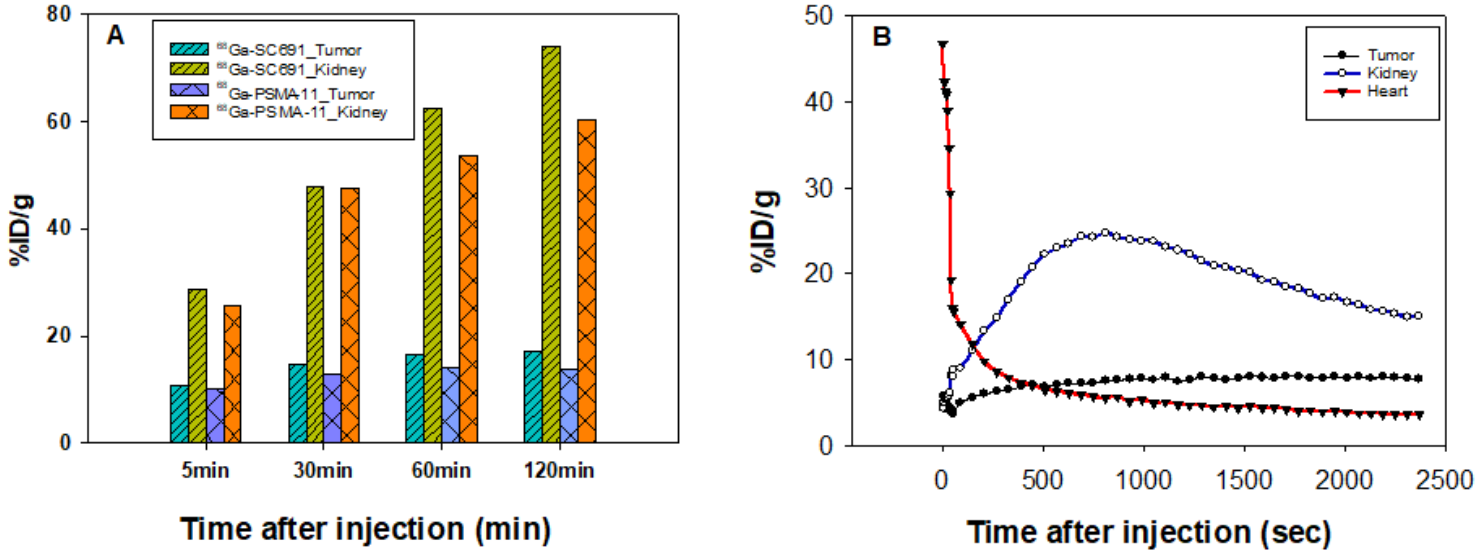

Figure 8

%ID/g obtained from whole-body coronal micro-PET/CT scan of an NOD/SCID male mice bearing LNCaP tumor xenografts (A), the tumor-targeting efficacy of 68Ga-SC691 was demonstrated by dynamic micro-PET scan(B).

Supplementary Files

This is a list of supplementary files associated with this preprint. Click to download.

- supportinginfo.docx
- Onlinefloatimage2.png